

# Electrical and Mechanical Compatible Design of 15 kW, 150,000 r/min Ultra-High-Speed PM Motor

Toshihiko Noguchi  
Graduate School of Integrated Science and Technology  
Shizuoka University  
Shizuoka, Japan  
noguchi.toshihiko@shizuoka.ac.jp

Kohei Fujita  
Graduate School of Integrated Science and Technology  
Shizuoka University  
Shizuoka, Japan  
fujita.kohei.14@shizuoka.ac.jp

**Abstract**— This paper describes an electrical and mechanical compatible design of an ultra-high-speed permanent magnet (PM) motor of which rated output power is 15 kW and rated speed is 150,000 r/min. In general, the electromagnetic design of the motor must be conducted under some mechanical constraints such as a rotor diameter and a rotor axial length, while the mechanical design is restricted by mechanical strength of the electromagnetic components such as a PM. In the paper, two candidates of the rotor structure have been investigated from the viewpoint of electrical and mechanical compatibility, i.e., a cylindrical hollow PM (standard SPM) rotor and a solid PM rotor with a titanium alloy sleeve. Both of the motors can achieve high efficiency over 96 % and high power density over 55 W/cm<sup>3</sup>, but the latter has a remarkable anti-demagnetization characteristic less than 1 %. Because the permeance of the solid PM rotor is extremely low, a lot of the leakage magnetic flux is generated in the motor, resulting in the eddy current losses of the metal shafts as well as the titanium alloy sleeve surrounding the solid PM. In order to investigate dependency of the shaft material onto the electromagnetic characteristics, three kinds of materials are employed for the shafts and are examined through 3-D electromagnetic analysis. As a result, stainless steel is the best choice for the shaft material and can satisfy the electrical and mechanical compatibility with high torque generation, high efficiency, high power density, high anti-demagnetization characteristic, and so forth.

**Keywords:** surface permanent magnet synchronous motor (SPMSM), high-speed motor, solid permanent magnet, demagnetization

## I. INTRODUCTION

Electrification of mechanically operated systems is widely and intensively spread to various industry sectors, home appliance product sectors, transportation and logistics sectors, and so forth. Electric machines play the most important role for the electrification of various kinds of industrial products. The most important points to develop electric machines are higher-power-density and fault-tolerant design as well as higher efficiency design. High-power motors are intensively developed to achieve higher-power-density in recent years, and permanent magnet synchronous motors (PMSMs) using rare earth PM are widely employed and are applied to various applications because of their excellent power density and efficiency. In order to enhance the motor output power, it is definitely necessary to deliver as high electromagnetic torque as possible and to rotate at as higher speed as possible under

some electrical and mechanical design constraints. In general, however, the higher-torque design tends to increase the machine volume, so higher-speed (higher-frequency operation) design is desirable and effective for further efficient downsizing of the machine.

High-speed motors have not only electrical but also mechanical design constraints in the design process, e.g., their rotor axial length is limited by the axial vibration and the resonance frequency, and their rotor diameter is limited by the circumference speed and the centrifugal force. In addition, generally accepted design concepts of the electric machines are not applicable to the high-speed motors because their downsized motor proportion makes it difficult to improve the electrical performance in the limited motor size without sacrificing the mechanical performance. Therefore, it is significantly important to discuss the electrical and mechanical compatible design of the high-speed motors.

Table I. Design specifications of 15-kW, 150,000-r/min PM motor.

Rated output power	Over 15 kW
Rated speed	150,000 r/min
Rated torque	Over 1 Nm
Rated efficiency	Over 95 %
Maximum power density	Over 50 W/cm <sup>3</sup>
Demagnetization rate	Within 1 %
DC bus voltage	Lower than 250 V
Rated current	77 A (over load 150%)
Maximum current	115 A
Rotor diameter	Smaller than 43.3 mm

Table II. Fundamental design outline of ultra-high-speed PM motor.

Motor type	Surface permanent magnet synchronous motor (SPMSM)
Number of phases	3 phases
Number of poles	2 poles
Stator configuration	Concentrated winding structure
Permanent magnet	N43TS Nd-Fe-B ( $B_r = 1.34$ T, $H_{CB} = 963$ kA/m, $BH_{max} = 350$ kJ/m <sup>3</sup> )
Electromagnetic steel plates	20HX1300 (0.2 mm thick, 0.54 $\mu\Omega$ m, $B_{max} = 1.5$ T)

Several ultra-high-speed PM motors have been developed by the authors, which feature the extremely wide air gap to reduce the synchronous inductance. It is possible to achieve the required output power specifications and to realize the excellent efficiency characteristic over 96 % with the wide-air-gap design, but the anti-demagnetization design is still difficult without sacrificing the outstanding electrical and mechanical performance of the motors. In the paper, the electrical and mechanical configuration of the rotor is mainly discussed, focusing on the anti-demagnetization characteristic of the PM mounted on the rotor. In addition, the rotor shaft material is investigated from the viewpoint of electromagnetic characteristics, and the appropriate material is chosen for the shaft to satisfy the electrical and mechanical requirements at the same time. The paper describes the electrical and mechanical compatible design of the 15-kW, 150,000-r/min ultra-high-speed PM motor on the basis of the above discussion.

## II. DESIGN TARGET AND BASIC DESIGN CONCEPT OF ULTRA-HIGH-SPEED PM MOTOR

### A. Design Target of Ultra-High-Speed PM Motor

TABLE I indicates a design target of the 15-kW, 150,000-r/min ultra-high-speed PM motor. The motor also has a 150-% momentary overload specification for the higher acceleration. The rotor diameter is limited under 43.3 mm so that the circumference speed of the rotor does not exceed the sonic velocity in the air because turbulence between the rotor and the concentrated winding stator may occur.

### B. Basic Design Concept of Ultra-High-Speed PM Motor

TABLE II shows designed parameters of the ultra-high-speed PM motor to be discussed in the paper. The cross section of the surface PM type motor is shown in Fig. 1, which is a typical surface permanent magnet synchronous motor (SPMSM). The rotor is actually reinforced by glass fiber or carbon fiber, which is wound around the rotor PM with epoxy resin. The SPM motor delivers only the magnet torque, but cannot deliver reluctance torque because of no saliency. The rotor diameter is too small (less than 43.3 mm) to employ interior permanent magnet (IPM) structure for the reluctance torque generation. Two-pole six-slot combination is employed to reduce an electrical frequency to drive the motor with an inverter. A NdFeB cylindrical shaped PM is mounted on the rotor shaft, of which maximum energy density is  $BH_{\max} = 350 \text{ kJ/m}^3$ ; hence the wide-air-gap structure is possible to employ, and the synchronous inductance can also dramatically be reduced with effective suppression of the permeance variation in the circumference direction. The stator is constituted with a concentrated winding six-tooth six-slot iron core for the purpose of reducing the leakage magnetic flux and the eddy current loss in the PM. The stator iron core employs 0.2-mm electromagnetic steel plates to reduce the iron loss, and 3-mm thick filets are on the tooth ends to avoid violent permeance variation in the circumference direction and to increase the winding coefficient to retrieve more PM magnetic flux.

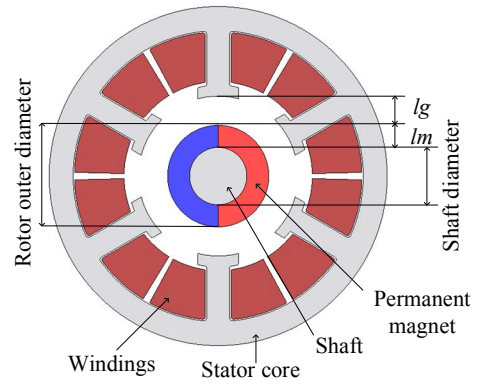


Fig. 1. Cross section of hollow magnet ultra-high-speed PM motor.

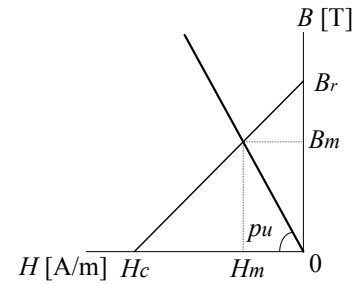


Fig. 2. B-H characteristic and operating point of permanent magnet.

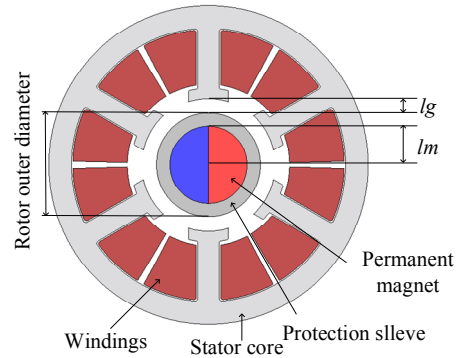


Fig. 3. Cross section of solid magnet ultra-high-speed PM motor.

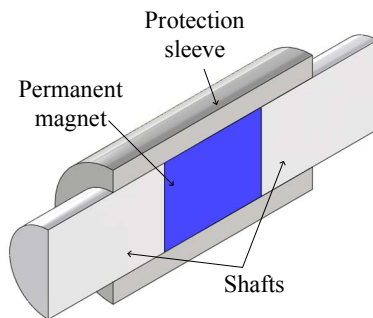


Fig. 4. Cross section of solid permanent magnet rotor.

### III. PRINCIPLE AND CONFIGURATION OF TWO-TYPE ULTRA-HIGH-SPEED PM MOTORS

#### A. Demagnetization Characteristic of Conventional SPM Configuration

An approach to improve the anti-demagnetization characteristic is to raise a permeance coefficient of the motor. The permeance coefficient is defined as the following equation, which determines the operating point of the PM:

$$p_u = \frac{l_m}{a_m} \frac{a_g}{K_c l_g} = \frac{l_m}{D_m - l_m} \frac{D_m + l_m}{K_c l_g}, \quad (1)$$

where

$p_u$  : permeance coefficient,

$l_m$  : PM thickness,

$a_m$  : average cross section area of PM,

$K_c$  : Carter's coefficient

$l_g$  : air gap length,

$a_g$  : average cross section area of air gap, and

$D_m$  : PM outer diameter.

As described previously, the cylindrical ring NdFeB PM is employed, and the air gap length is much longer than that of the standard PM motor, i.e., almost same as the thickness of the PM. On the other hand, it is indispensable to enlarge the rotor shaft diameter to make the resonant frequency as high as possible, resulting in prevention of the mechanical shaft vibration. Therefore, the SPM type ultra-high-speed motor must have the low permeance coefficient due to the low value of  $l_m$ , which is limited by both of the rotor shaft diameter and the rotor outer diameter. The thinner PM makes the anti-demagnetization characteristic worse.

#### B. Demagnetization Characteristic of Conventional SPM Configuration

Keeping the wide air gap configuration to make the synchronous inductance as low as possible, a new rotor configuration is discussed, where the rotor is fully filled with the PM and has no shaft. Figure 3 illustrates a cross section of the ultra-high-speed PM motor, of which rotor is filled with a solid NdFeB PM. As can be seen in the figure, it is possible to maximize  $l_m$  and to minimize  $a_m$ ; thus the permeance coefficient can be enlarged without sacrificing the inherent wide air gap.

Figure 4 illustrates an axial cross section of the solid PM rotor. This configuration of the rotor does not allow having the shaft in the PM, so it is necessary to reinforce the solid PM rotor with a stiff and robust metal sleeve in order to prevent the rotor from scattering. By taking advantage of the mechanical reinforcement by the metal sleeve, it is possible to allocate the metal shaft and the solid PM rotor on the identical axis, and to joint them tightly. A titanium alloy is employed for the metal sleeve because the mechanical strength is relatively high, and the titanium alloy sleeve makes it possible to connect the shafts to the both ends of the solid PM rotor and to reinforce the rotor at the same time. Since the titanium alloy has as low

Table 1. Design parameters and major specifications of motor models.

Motor model	# 1 (hollow)	# 2 (solid)
Rotor outer diameter	37.2 mm	39.0 mm
$l_m$	8.1 mm	14 mm
$l_g$	10.7 mm	5.55 mm
Permeance coefficient	1.1	3.3
Number of winding turns	22	22
Winding space factor	50.8 %	50.8 %
Current density	4.78 A (rated operation)	4.78 A (rated operation)
Protection sleeve	Glass fiber (0 $\Omega$ m)	Titanium alloy (2.3 $\mu\Omega$ m)
Stator winding resistance	5.5 m $\Omega$	5.3 m $\Omega$
Stator winding inductance	37 $\mu$ H	38 $\mu$ H
Efficiency at rated operating point	97.4 %	96.9 %
Maximum power density	57.9 W/cm <sup>3</sup>	60.4 W/cm <sup>3</sup>

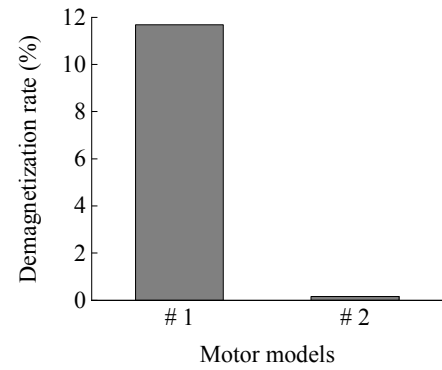


Fig. 5. Comparison of demagnetization characteristics.

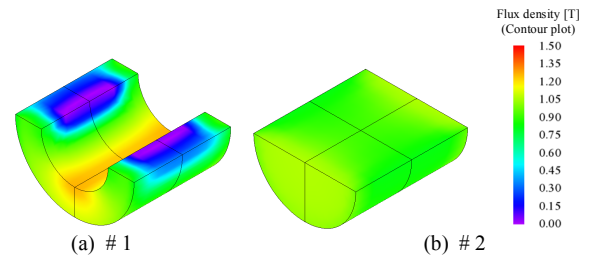


Fig. 6. Flux density distribution of permanent magnets on demagnetized situation.

permeability as air, it is possible to reduce the synchronous inductance because the rotor including the protection sleeve can be regarded as air. This great feature contributes to drive the motor at a lower terminal voltage.

In the following sections, the SPM type motor #1 with the cylindrical hollow PM shown in Fig. 1, and the motor #2 of which rotor is fully filled by the PM shown in Figs. 3 and 4 are electrically compared. An electromagnetic analysis software JMAG-Designer 18.0<sup>TM</sup> is used to evaluate the designed motor performances.

#### IV. CONDITIONS OF ELECTROMAGNETIC ANALYSIS AND EVALUATION

Design parameters and the major specifications of the two-type motors are listed in TABLE III. Both motors have a flat proportion, and have stator overhang of 1 mm for each end of the stator iron core to receive as much PM magnetic flux as possible. The synchronous inductance of the two motors is reduced down to approximately 37 uH owing to the wide air gap configuration. It is considered, however, that the #2 motor with the solid PM rotor has much more leakage inductance because its inductance is almost same as that of the #1 motor regardless of the no-shaft configuration in the PM. The magnetic flux density in the stator back yoke and the stator teeth is approximately 1.4 T for both motors, and the two motors have achieved high efficiency over 96 % and high power density over 55 W/cm<sup>3</sup>.

The anti-demagnetization characteristic and the power loss of the rotor are the most important performance indexes to evaluate the two motors. It is desirable to reduce the demagnetization rate less than 1 %, and to control the copper loss and the iron loss to maximize the efficiency at the rated operating point. In the following section, the electromagnetic analysis results are compared between the two motors from the viewpoints of the demagnetization characteristics, the power losses, and the maximum efficiency operating points. The demagnetization characteristics are examined under the conditions of 200-°C PM temperature and the maximum negative d-axis current, and the no-load electromotive forces (e.m.f.) before the demagnetization at room temperature and after the demagnetization described above are compared. When the power losses and the efficiency are discussed, the motor temperature is assumed to be 75 °C. The maximum efficiency can be obtained when the equation below is satisfied:

$$W_s + W_r = W_c, \quad (2)$$

where

- $W_s$  : stator iron core loss,
- $W_r$  : rotor iron core loss, and
- $W_c$  : stator winding copper loss.

It is found from this equation that the maximum efficiency can be obtained if the iron losses and the copper loss are almost same. The maximum efficiency operating points are evaluated from the viewpoint of this condition.

Figure 5 shows demagnetization characteristics of the two motors, and the magnetic flux density distributions after the demagnetization are shown in Fig. 6. It is confirmed from Fig. 5 that the demagnetization rate of #2 motor is less than 1 % of #1 motor. This significant difference can be observed in the demagnetization areas in the PMs as shown in Fig. 6. Therefore, the solid PM rotor is remarkably effective to prevent the demagnetization, compared with the standard SPM rotor.

The total power losses and their analysis results are indicated in Fig. 7, where the iron loss analysis results are shown in Fig. 8 and the eddy current loss of the titanium alloy sleeve is shown in Fig. 9, respectively. The all results are estimated at the rated operating point. It is found from Fig. 7

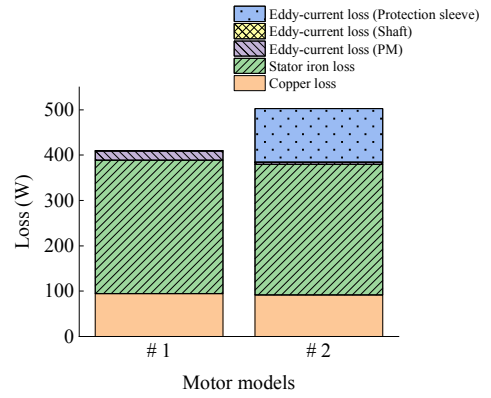


Fig. 7. Comparison of total losses at rated operation and loss analysis results.

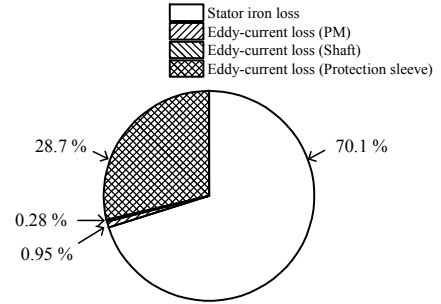


Fig. 8. Analysis result of iron loss of #2 motor at rated operation.

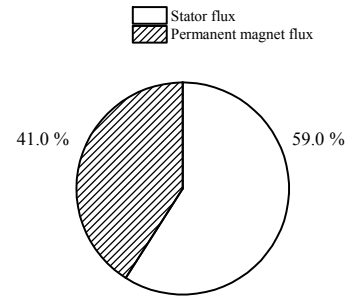


Fig. 9. Detail of eddy-current loss in protection sleeve.

that the total power loss of #1 motor is less than that of #2 motor because of the eddy current loss caused in the titanium alloy sleeve on the rotor. The percentage of the eddy current loss in the titanium alloy sleeve of the #2 motor is 28.7 % (117.8 W), and is a dominant cause of efficiency degradation. The reason why the eddy current is generated in the titanium alloy sleeve is a permeance variation caused by the concentrated-winding-structure based slot ripples. According to Fig. 9, it can be found that the eddy current loss caused by the PM magnetic flux is 41 %, and that caused by the stator magnetic flux is 59 %. The permeance variation of the motor is basically small because of the wide air gap, but the stator leakage magnetic flux easily interlinks to the titanium alloy sleeve, which is the major reason of the eddy current generation. The temperature rise of the PM caused by the eddy

current loss in the titanium alloy sleeve may be a great concern, but the specific heat and the thermal conductivity of the titanium alloy are very small. Therefore, the possibility of the thermal demagnetization is considered to be very low. The efficiencies of the two motors are almost same because the ratios between the iron losses and the copper loss are very similar as shown in Fig. 7.

## V. DISCUSSION ON SHAFT MATERIAL OF SOLID PM ROTOR

### A. Electromagnetic Characteristics Depending on Rotor Shaft Material

Figure 10 illustrates the stator magnetic flux behavior in the ultra-high-speed PM motor with the solid PM rotor. The rotor shaft material influences the electromagnetic characteristics of the motor because the leakage magnetic flux is not negligible as described in the previous section. If the permeability of the shaft is higher than that of the PM, the stator magnetic flux linking to the rotor is reduced because much of the flux goes to the shaft. In addition, the pole pair makes short circuits in the three-dimensional magnetic paths through the shaft, which increases the leakage magnetic flux of the PM. These leakage magnetic fluxes do not contribute to generate the average torque, but improve the anti-demagnetization characteristic as a result. If the permeability of the shaft is as low as air, the stator magnetic flux linking to the rotor is relatively increased because there is not significant difference in the permeability of the rotor and the shaft. The leakage magnetic flux between the PM pole pair through the shaft is reduced, resulting in improvement of the average torque generation but in deterioration of the demagnetization characteristic. In the following section, the electromagnetic characteristics are discussed from the viewpoint of a trade-off between the average torque and the demagnetization characteristic, picking up three kinds of shaft materials.

### B. Electromagnetic Analysis Conditions and Methods

Assuming that one of the three-kind metal materials is employed as the shafts, i.e., (a) S45C, (b) SUS304, and (c) titanium alloy, the average torque, the demagnetization characteristics, and the efficiency characteristics are examined. An initial relative permeability of S45C is the highest and 1846.2, and that of the titanium alloy is the lowest and almost 1 same as air. The demagnetization characteristics are examined at the PM temperature of 200-°C and the maximum negative d-axis current is given to the motor. The no-load e.m.f. before the demagnetization at room temperature and after the demagnetization is compared. When the power losses and the efficiency are examined, it is assumed that the motor temperature is 75 °C.

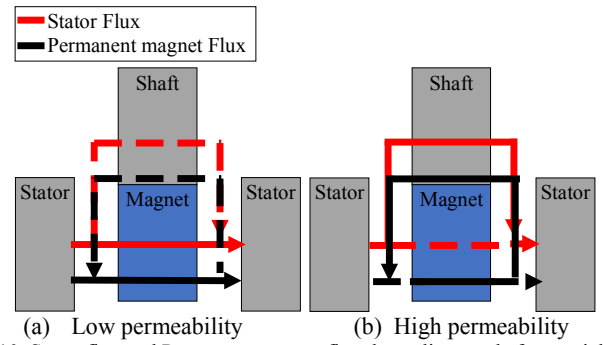


Fig. 10. Stator flux and Permanent magnet flux depending on shaft materials.

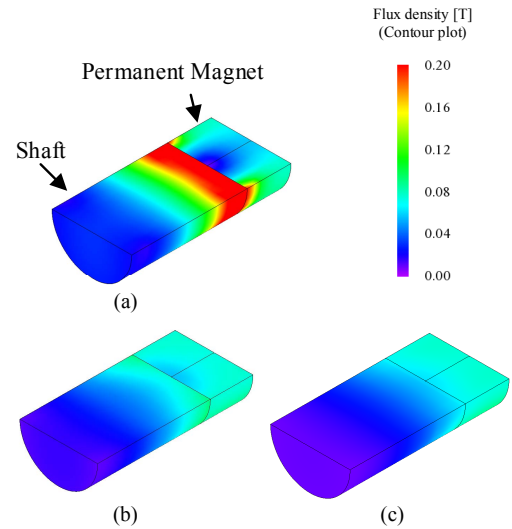


Fig. 11. Stator flux density distribution depending on shaft materials.

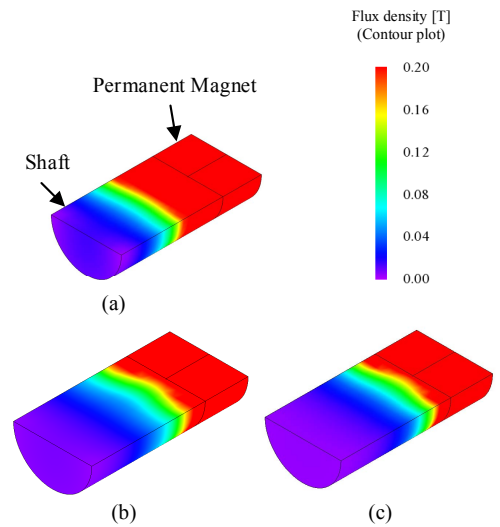


Fig. 12. Permanent magnet flux density distribution depending on shaft materials.

Table IV. Electrical characteristics depending on shaft materials.

Motor models	Shaft material	Initial relative permeability	Demagnetization rate	Average torque	Total loss	Eddy-current loss (Shaft)	Efficiency
a	S45C	1846.2	0.53 %	1.10 Nm	790.3 W	1.2 W	95.62%
b	SUS304	2.1	0.16 %	1.48 Nm	816.3 W	2.2 W	96.60%
c	Titanium alloy	1.0	1.42 %	1.49 Nm	815.5 W	4.6 W	96.64%

### C. Comparison of Analysis Results

TABLE IV lists the analysis results depending on the shaft materials. Figure 11 shows the stator magnetic flux density distribution of the three cases. It can be found that the anti-demagnetization rate of (b) is almost 1/3 of that of (c) because the stator magnetic flux linking to the rotor PM is reduced by the leakage magnetic flux through the shaft. On the other hand, (a) is much better than (b) in terms of the anti-demagnetization characteristic because the leakage magnetic flux to the S45C shaft is increased and the counter magnetic flux against the PM is reduced.

On the other hand, the magnetic flux density distributions of the rotor are indicated for the three cases. There is about 26-% difference in the average torque between (a) and (c), but (b) and (c) can deliver almost the same average torque. As can be observed in Fig. 12, the magnetic flux density of the shaft in the case of (a) is much higher than that of (b) and (c), which implies that the leakage magnetic flux between the PM poles through the shaft is increased.

The efficiency of (a) is slightly lower than (b) and (c). The total power loss and the average torque of (a) is approximately 4 % lower and approximately 26 % lower than those of (b) and (c), respectively. Although the total power loss is improved by introducing the S45C shaft in the case (a), the average torque deterioration detrimentally affects to the efficiency, which is caused by the excessive leakage magnetic flux through the shaft.

## VI. CONCLUSION

This paper has described an electrical and mechanical compatible design of an ultra-high-speed PM motor, of which rated output power is 15 kW and rated speed is 150,000 r/min. In order to satisfy not only the ratings but also high efficiency over 96 % and high power density over 55 W/cm<sup>3</sup>, the two types of the PM motors are investigated, i.e., a motor with a cylindrical hollow PM (standard SPM) rotor and the other motor with a solid PM rotor. It has been confirmed that both of the motors can attain the design target but that the solid PM rotor configuration makes it possible to improve an anti-demagnetization characteristic at the same time. By introducing the solid PM rotor structure, the total power loss increases by approximately 20 %, which is mainly caused by a titanium alloy sleeve, but the demagnetization rate can be dramatically reduced down to less than 1 %.

However, the motor with the solid PM rotor has another unavoidable problem, which is the leakage magnetic flux caused by an extremely low permeance of the solid PM and the protective titanium alloy sleeve. Particularly, it has been found

that the stator magnetic flux affects the eddy current in the metal shafts as well as the titanium alloy sleeve surrounding the solid PM. In the paper, three kinds of metal materials for the shafts have been investigated, i.e., steel S45C, stainless steel SUS304, and titanium alloy, and dependency of the materials onto the electromagnetic characteristics has been examined through the 3-D electromagnetic analysis. As a result, stainless steel SUS304 is the best choice for the shafts from the viewpoints of the average torque, the efficiency, the anti-demagnetization characteristic, and so forth. It has been found in the investigation that the average torque characteristic and the anti-demagnetization characteristic have a trade-off relationship, depending on the permeability of the shaft material.

For the future work, it is required to reduce the eddy current loss of the protection sleeve on the solid PM rotor, which occupies 28.7 % of the total power loss, and to improve the efficiency further without sacrificing the anti-demagnetization characteristic.

## REFERENCES

- [1] Hirokatsu Katagiri, Hiroyuki Sano, Kazuki Semba, Noriyo Mimura, and Takashi Yamada "Fast Calculation of AC Copper Loss for High Speed Machines by Zooming Method," IEEJ J. Industry Applications, vol. 6, no. 6, pp. 395-400, 2017.
- [2] Kenta Yamano, Shigeo Morimoto, Masayuki Sanada, and Yukinori Inoue "Design of Surface Permanent Magnet Synchronous Motor Using Design Assist System for PMSM," IEEJ J. Industry Applications, vol. 6, no. 6, pp. 409-415, 2017.
- [3] K. Sakai, T. Tokumasu, and K. Itou, "Magnetic Field Analysis of a Super-High-Speed Permanent Magnet Motor with a New Rotor," Journal of the Japan Society of Applied Electromagnetics, Vol. 4, no. 3, pp. 40-45, 1996.
- [4] T. Noguchi, Y. Takata, Y. Yamashita, Y. Komatsu, and S. Ibaraki, "220000 r/min, 2-kW PM Motor Drive for Turbocharger," IEEJ Trans. IA, vo. 125, no. 9, pp. 854-851, 2005.
- [5] T. Noguchi, T. Komori, "Eddy-Current Loss Analysis of Copper-Bar Windings of Ultra High-Speed PM Motor," 3rd International Conference on Electrical Systems for Aircraft, Railway, Ship Propulsion and Road Vehicles, Aachen, Germany, (2015-2).
- [6] K. Ogata, and T. Noguchi, "Efficiency Improvement of 3-kW, 150,000-r/min Ultra High-Speed PM Motor Focusing on Conductor Eddy-Current Loss," IEEJ Technical Meeting on Motor drive Rotating Machinery, Automotive Machinery, MD-18-074, RM-18-060, VT-18-015, (2018-9).
- [7] T. Wada, and T. Noguchi, "Optimum Design Focused on Efficiency and Power Density of 1.5-kW, 150,000-r/min PM Motor Fed by Low-Voltage Power Supply," IEEJ Technical Meeting on Semiconductor Power Converter and linear drive, SPC-09-174, LD-09-064, (2009-12).
- [8] K. Fujita, and T. Noguchi, "Study on propotion of 15 kW, 150,000 r/min PM motor," IEEJ Annual National Conference, 5-031, (2019-3).